Motion Planning and Control of UVMS: A Unified Dynamics-based Approach

Tarun Kanti Podder
Research & Development Engineering
Monterey Bay Aquarium Research Institute
Moss Landing, CA 95039, USA
tarun@mbari.org

Nilanjan Sarkar
Department of Mechanical Engineering
Vanderbilt University, Nashville
Tennessee, TN 37235, USA
nilanjan.sarkar@vanderbilt.edu

Abstract

In this paper, we present a new unified motion planning algorithm for autonomous Underwater Vehicle-Manipulator Systems (UVMS) that considers the variability in dynamic bandwidth of such a complex system and generates both kinematically admissible and dynamically feasible reference trajectories. Additionally, this motion planning algorithm exploits the inherent kinematic redundancy of the system and provides reference trajectories that can accommodate thruster and actuator faults and saturation, and minimizes hydrodynamic drag. This unified algorithm is verified by extensive computer simulations and the results are presented here.

1. Introduction

Trajectory planning is one of the most challenging problems in robotics [1]. Traditionally, trajectory planning problem is formulated as a kinematic problem and therefore, the dynamics of the robotic system is neglected [2]. Although the kinematic approach to the trajectory planning has yielded some very successful and results, they are essentially incomplete as the planner does not consider dynamics while generating the reference trajectory. As a result, the reference trajectory may be *kinematically admissible* but may not be *dynamically feasible*.

In the past several years, researchers have developed various trajectory planning methods for robotic systems considering different kinematic and dynamic criteria such as obstacle avoidance, singularity avoidance, time minimization, torque optimization, energy optimization, and other objective functions [3-18]. A robotic system that has more than 6 dof (degrees-of-freedom) is termed as kinematically redundant system. For a kinematically redundant system, the mapping between task-space trajectory and the joint-space trajectory is not unique. It admits infinite number of joint-space solutions for a given task-space trajectory. There are various mathematical tools such as Moore-Penrose Generalized Inverse, which map the desired Cartesian trajectory into the corresponding joint-space trajectory for a kinematically redundant system. Researchers have developed various trajectory planning methods for redundant systems [1,3-5,9]. Kinematic approach of motion planning has been reported in [1-5]. In [3], Zhou and Nguyen formulated optimal joint-space trajectories for kinematically redundant manipulators by applying Pontryagin's Maximum Principle. Siciliano [4] has proposed an inverse kinematic approach for motion planning of redundant spacecraft-manipulator system. In [5], Antonelli and Chiaverini have used pseudoinverse method for task-priority redundancy resolution for a Underwater Vehicle Manipulator System (UVMS) using a kinematic approach.

Several researchers [6-14], on the other hand, have considered dynamics of the system for trajectory planning. In [6], Vukobratovic and Kircanski proposed an inverse problem solution to generate nominal join-space trajectory considering the dynamics of the system. In [7], Bobrow presented the Cartesian path of the manipulator with a B-spline polynomial and then optimized the total path traversal time satisfying the dynamic equations of motion. Shiller and Dubowsky [8] presented a time-optimal motion planning method considering the dynamics of the system. In [9], Shin and McKay proposed a dynamic programming approach to minimize the cost of moving a robotic manipulator. Recently, Hirakawa and Kawamura [10] have proposed a method to solve trajectory generation problem for redundant robot manipulators using the variational approach within B-spline function to minimize the consumed electrical energy. Saramago and Steffen [11] have formulated off-line joint-space trajectories to optimize raveling time and minimize mechanical energy of the actuators using spline functions. In [12], Macfarlane et al. have developed and implemented a real-time jerk-bounded trajectory using concatenated quintic polynomials. Faiz and Agrawal [13] have proposed a trajectory planning scheme that explicitly satisfy the dynamic equations and the inequality constraints prescribed in terms of joint variables. Motion planning of land-based mobile robotic systems has been reported in [14-15].

Majority of the trajectory planning methods available in the literature that considered the dynamics of the system are formulated for land-based robots.

0-933957-31-9

They have either optimized some objective functions related to trajectory planning satisfying dynamic equations or optimized energy functions. Moreover, for the land-based robotic system, the dynamics of the system is either homogeneous or very close to homogeneous. On the other hand, most of the trajectory planning methods that have been developed for space and underwater robotic systems use the pseudoinverse approach that neglects the dynamics of the system [4-5,16-18].

In this research we propose a new trajectory planning methodology that generates a kinematically admissible and dynamically feasible trajectory for kinematically redundant systems whose subsystems have greatly different dynamic responses. We consider the trajectory planning of underwater robotic systems, i.e., *autonomous UVMS* as an application to the proposed theoretical development. A UVMS is composed of a *6* dof autonomous underwater vehicles (AUV) and one (or more) *n* dof robotic manipulator(s). Generally, the dynamic response of the vehicle is an order of magnitude slower than that of the manipulator(s). Therefore, a UVMS is a kinematically redundant heterogeneous dynamic system for which the trajectory planning methods available in the literature are not directly applicable. For example, when the joint-space description of a robotic system is determined using pseudoinverse, all joints are implicitly assumed to have same or similar dynamic characteristics. Therefore, the traditional trajectory planning approaches may generate such reference trajectories for a UVMS that either it may not be able to track or while tracking, it may consume exorbitant amount of energy.

Additionally, in this research, we exploit the kinematic redundancy of a UVMS and unify it to the dynamically feasible trajectory generation scheme to develop reference trajectories that can accommodate thruster and actuator faults, saturation and provide a minimum drag trajectory for a given task. All these performance criteria are important for *autonomous* underwater operations. They provide a fault-tolerant, reduced energy consuming autonomous operation framework.

2. Theoretical Development

2.1 Dynamics-Based Trajectory Planning

In this section, we present a trajectory planning algorithm that accounts for different bandwidth characteristic of a dynamic system. First, we present the algorithm for a general *s*-bandwidth dynamic system. Then we improvise this algorithm for the application to a UVMS.

Let us assume that we know the natural frequency of each subsystem of the heterogeneous dynamic system. This will give a measure of the dynamic response of each subsystem. Let these frequencies be ω_i, $i = 1,2,\cdots\cdots,s$.

We approximate the task space trajectory using Fourier series and represent it in terms of the summation of several frequencies in ascending order.

$$x_{d_{6\times1}}(t) = f_{6\times1}(t) = a_0 + \sum_{r=1}^{\infty} a_r \cos(r\pi t/L) + \sum_{r=1}^{\infty} b_r \sin(r\pi t/L) \quad (1)$$

where a_0, a_r, b_r are the coefficients of Fourier series and are represented as 6×1 column vectors, $r/2L$ is the frequency of the series and *2L* is the time period.

Now we truncate the series at a certain value of *r* (assuming *r* to be sufficiently large) so that it can represent the task space trajectory reasonably. We rewrite the task-space trajectory in the following form:

$$x_{d_{6\times1}}(t) = f_{6\times1}(t) = f_1(t) + f_2(t) + \cdots\cdots + f_{p_1}(t) \quad (2)$$

where $f_1(t) = a_0 + a_1\cos(\pi t/L) + b_1\sin(\pi t/L)$, and $f_j(t) = a_j\cos(j\pi t/L) + b_j\sin(j\pi t/L)$ for $j = 2,3,..., p_1$.

We then use these truncated series as the reference task-space trajectory and map them into the desired (reference) joint-space trajectory by using weighted pseudoinverse method as follows:

$$\dot{q}_{d_j} = J^{+}_{W_j}\dot{x}_{d_j} \quad (3)$$

$$\ddot{q}_{d_j} = J^{+}_{W_j}(\ddot{x}_{d_j} - \dot{J}\dot{q}_{d_j}) \quad (4)$$

where $\dot{q}_{d_j}$ and $\ddot{q}_{d_j}$ are the joint-space velocity and acceleration corresponding to the task-space velocity $\dot{x}_{d_j} = d(f_j(t))/dt$ and acceleration $\ddot{x}_{d_j} = d^2(f_j(t))/dt^2$ for $j = 1,2,..., p_1$. $J^{+}_{w_j} = W_j^{-1}J^T(JW_j^{-1}J^T)^{-1}$ is the weighted pseudoinverse of Jacobian, *J*, and $W_j = diag(h_{1_j},......., h_{(6+n)_j})$ is a diagonal weight matrix.

In our proposed scheme we use weighted pseudoinverse technique in such a way that it can act as a filter to remove the propagation of undesirable frequency components from the task-space trajectory to the corresponding joint-space trajectory for a particular subsystem. This can be done by putting suitable zeros in the diagonal entries of the W_j^{-1} matrix in Eq. (3) and Eq. (4). We leave the other elements of W_j^{-1} as unity. We consider two cases for such a frequency-wise decomposition as follows:

Case I – Partial Decomposition:

The segments of the task-space trajectory having frequencies ω_t $(\omega_t \le \omega_i)$ will be taken by all subsystems that have natural frequencies greater than ω_t up to the maximum bandwidth subsystem. To give an example, for a UVMS, the lower frequencies will be shared by both the vehicle and the manipulator, whereas the higher frequencies will be solely taken care of by the manipulator.

Case II- Total Decomposition:

In this case, we partition the total system into several frequency domains, starting from the low frequency subsystem to the very high frequency subsystem. We then allocate a particular frequency component of the task-space trajectory to only those subsystems that belong to the frequency domain just higher than the task-space component to generate joint-space trajectory. For a UVMS, this means that the lower frequencies will be taken care of by the vehicle alone and the higher frequencies by the manipulator alone.

To improvise the general algorithm for a *6+n* dof UVMS, we decompose the task-space trajectory into two components as follows:

$$f(t) = f_{11}(t) + f_{22}(t) \tag{5}$$

where $f_{11}(t) = a_0 + \sum_{r=1}^{r_1} a_r \cos(r\pi t / L) + \sum_{r=1}^{r_1} b_r \sin(r\pi t / L)$

$f_{22}(t) = \sum_{r=r_1+1}^{r_2} a_r \cos(r\pi t / L) + \sum_{r=r_1+1}^{r_2} b_n \sin(r\pi t / L)$, r_1 and r_2 $(r_2 = p_1)$ are suitable finite positive integers. Here, $f_{11}(t)$ consists of lower frequency terms and $f_{22}(t)$ has the higher frequency terms.

Now the mapping between the task-space variables and the joint-space variables are performed as

$$\ddot{q}_{d_1} = J^{+}_{W_1}(\ddot{x}_{d_1} - \dot{J}\dot{x}_{d_1})\,;\ \ddot{q}_{d_2} = J^{+}_{W_2}(\ddot{x}_{d_2} - \dot{J}\dot{x}_{d_2}) \tag{6}$$

$$\ddot{q}_d = \ddot{q}_{d_1} + \ddot{q}_{d_2} \tag{7}$$

where $W_i \in \Re^{(6+n)\times(6+n)}$ is the weight matrix, $\ddot{q}_d \in \Re^{(6+n)}$ is the joint-acceleration and $J^{+}_{wi} = W_i^{-1}J^T(JW_i^{-1}J^T)^{-1}$ for (*i=1,2*). We have considered the weight matrices for two types of decompositions as follows:

For Case I – Partial decomposition:

$W_1 = diag(h_1, h_2, ..., h_{6+n})$; $W_2 = diag(0,....,0, h_7, ..., h_{6+n})$

For Case II- Total decomposition:

$W_1 = diag(h_1, ..., h_6, 0, ..., 0)$; $W_2 = diag(0,....,0, h_7, ..., h_{6+n})$

The weight design is further improved by incorporating the damping into the trajectory generation by designing the diagonal entries of the weight matrix as $h_i = f(\zeta_i)$, where ζ_i (*i=1,…...,6+n*) is the damping ratio of the particular dynamic subsystem.

2.2 Fault Tolerant Decomposition

An autonomous UVMS is expected to function in a hazardous and unstructured underwater environment. Therefore, the fault-tolerant property to overcome thruster/ actuator breakdown is important. In general, there are more thrusters and actuators than what is minimally required for the specific dof that a UVMS is designed for. Here, we develop an approach to exploit the thruster and actuator redundancy to accommodate thruster/actuator faults during operation.

The dynamic equations of motion of UVMS can be expressed as follows:

$$M_b(q_m)\dot{w} + C_b(q_m, w)w + D_b(q_m, w)w + G_b(q) = \tau_b \tag{8}$$

where the subscript *'b'* denotes the corresponding parameters in body-attached frame of the UVMS. $M_b(q_m) \in \Re^{(6+n)\times(6+n)}$ is the inertia matrix including the added mass matrix, $C_b(q_m, w) \in \Re^{(6+n)\times(6+n)}$ is the matrix of centrifugal and Coriolis forces/moments including terms due to added mass, $D_b(q_m, w) \in \Re^{(6+n)\times(6+n)}$ is the matrix of drag forces/moments, $G_b(q) \in \Re^{(6+n)}$ is the vector of gravity and buoyancy forces/moments and $\tau_b \in \Re^{(6+n)}$ is the vector of forces/moments acting on UVMS. $w = [w_1, ..., w_{6+n}]^T$ is the quasi velocity vector and $q = [q_v, q_m]^T$ is the vector of generalized coordinates where $q_v = [q_1, ..., q_6]^T$ and $q_m = [q_7, ..., q_{6+n}]^T$.

In order to relate the generalized force vector τ_b with the individual thruster/actuator force/torque, let us consider a UVMS which has *p* thrusters and actuators where, in general, $p \geq (6+n)$. In such a case, we can write

$$\tau_b = EF_t \tag{9}$$

where $E_{(6+n)\times p}$ *thruster configuration matrix* and $F_{t_{p\times 1}}$ is the thruster/actuator force/torque.

Substituting Eq. (9) into Eq.(8) and performing algebraic manipulation we get,

$$\dot{w} = M_b^{-1}(EF_t - \xi_b) \tag{10}$$

where $\xi_b = C_b(q_m, w)w + D_b(q_m, w)w + G_b(q)$.

Eq. (8) is represented in the body-attached frame of the UVMS because it is convenient to measure and control the motion of the UVMS with respect to the moving frame. However, the integration of the angular velocity vector does not lead to the generalized coordinates denoting the orientation of the UVMS. In general, we can relate the derivative of the generalized coordinates and the velocity vector in the body-attached frame by the following linear transformation:

$$\dot{q} = Bw \tag{11}$$

where $B_{(6+n)\times(6+n)}$ is a transformation matrix.

Differentiation of Eq. (11) leads to the following acceleration relationship:

$$\ddot{q} = B\dot{w} + \dot{B}w \tag{12}$$

Now, combining Eq. (10) and Eq. (12) we get,

$$\ddot{q} = \eta F_t + \lambda \tag{13}$$

where $\eta_{(6+n)\times p} = BM_b^{-1}E$ and $\lambda_{(6+n)\times 1} = \dot{B}w - BM_b^{-1}\xi$.

From Eq. (13), using weighted pseudoinverse technique we can get a least-norm solution to thruster/actuator force/torque as

$$F_t = \eta_W^+ (\ddot{q} - \lambda) \tag{14}$$

where $\eta_W^+ = W^{-1}\eta^T(\eta W^{-1}\eta^T)^{-1}$ is the weighted pseudoinverse of η and $W = diag(h_1, h_2, ..., h_p)$ is the weight matrix.

Now, we construct a *thruster fault matrix*, $\psi_{p\times p} = W^{-1}$, with diagonal entries either 1 or 0 to capture the fault information of each individual thruster/actuator. If there is any thruster/actuator fault we introduce 0 into the corresponding diagonal element of ψ, otherwise it will be 1. We can also rewrite Eq. (14) in terms of thruster fault matrix, ψ, as

$$F_t = \psi\eta^T(\eta\psi\eta^T)^{-1}(\ddot{q} - \lambda) \tag{15}$$

Eq. (15) provides us the fault tolerant allocation of thruster/actuator force/torque, F_t. More detailed discussion on this topic can be found in [19-20].

2.3 Saturation Limit

In the previous section we have derived Eq. (15) for desired thruster/actuator force/torque allocation that allows the operation of the UVMS with faults. However, they cannot guarantee that the desired allocated force/torque will remain within the saturation limit. We, therefore, propose to use a dynamic state feedback technique [21] to generate thruster/actuator force/torque that stay within the saturation limit.

We differentiate the output Eq. (13) to obtain

$$\dddot{q} = \eta \dot{F}_t + \dot{\eta} F_t + \dot{\lambda} = \eta\nu + \gamma \tag{16}$$

where $\gamma = \dot{\eta} F_t + \dot{\lambda}$.

Now, we consider the following control law

$$\nu = \eta_{WF}^+ [\dddot{q}_d + K_1(\ddot{q}_d - \ddot{q}) + K_2(\dot{q}_d - \dot{q}) + K_3(\dot{q}_d - \dot{q})] - \gamma \tag{17}$$

where $\eta_{WF}^+ = W_F^{-1}\eta^T(\eta W_F^{-1}\eta^T)^{-1}$, K_1 is the acceleration gain, K_2 is the velocity gain and K_3 is the position gain. The diagonal elements of the weight matrix, $W_F = diag(\hbar_1, \hbar_2 ...., \hbar_p)$, are computed from the thruster/actuator saturation limits as follows:

We define a function of thruster and actuator force and torque variables as

$$H(F_t) = \sum_{i=1}^{p} \frac{1}{C_i} \frac{(F_{t_{i,\max}} - F_{t_{i,\min}})}{(F_{t_{i,\max}} - F_{t_i})(F_{t_i} - F_{t_{i,\min}})} \tag{18}$$

where $F_{t_{i,\max}}$ and $F_{t_{i,\min}}$ are the upper and lower limits of thrust/torque of the *i*-th thruster/actuator, and C_i is a positive quantity which is determined from the damping property of the system dynamics. Then, differentiating Eq. (18), we obtain

$$\frac{\partial H(F_t)}{\partial F_{t_i}} = \frac{(F_{t_{i,\max}} - F_{t_{i,\min}})^2 (2F_{t_i} - F_{t_{i,\max}} - F_{t_{i,\min}})}{C_i \; (F_{t_{i,\max}} - F_{t_i})^2 (F_{t_i} - F_{t_{i,\min}})^2} \tag{19}$$

Then, we define: $\hbar_i = 1 + \left|\partial H(F_i)/\partial F_i\right|$ (20)

From the above expression (19), we notice that $\partial H(F_t)/\partial F_{t_i}$ is equal to zero when the *i*-th thruster/actuator is at the middle of its range, and becomes infinity at either limits. Thus, $\hbar_i$ varies from 1 to infinity if the *i*-th thrust goes from middle of the range to its limit. If the *i*-th thrust/torque approaches its limit, then $\hbar_i$ becomes very large and the corresponding element in W_F^{-1} goes to zero and the *i*-th thruster/actuator avoids saturation.

Depending upon whether the thruster/actuator is approaching toward or departing from its saturation limit, $\hbar_i$ can be redefined as $\hbar_i = 1 + \left|\partial H(F_i)/\partial F_i\right|$ when $\Delta\left|\partial H(F_i)/\partial F_i\right| \geq 0$ (i.e., the thruster/actuator force/torque is approaching toward its limit), and $\hbar_i = 1$ when $\Delta\left|\partial H(F_i)/\partial F_i\right| \leq 0$ (i.e., the thruster/ actuator force/torque is departing from its limit). Finally, the desired thruster/actuator force/torque vector, F_t, that is guaranteed to stay within the saturation limit and it is obtained by the integration of the new input ν given by Eq. (17).

Substituting Eq. (17) into Eq. (16) and denoting $e = q_d - q$, we obtain the following error equation in joint-space

$$\dddot{e} + K_1\ddot{e} + K_2\dot{e} + K_3 e = 0 \tag{21}$$

Thus, for positive values of the gains, K_1, K_2 and K_3, the joint-space error dies down to zero asymptotically, as time goes to infinity.

Now, to incorporate both the fault and the saturation information in control Eq. (17), we define a *fault-saturation matrix,* $\Gamma_{p\times p} = W_F^{-1}$, having diagonal elements either $1/\hbar_i$ or zero. Whenever there is any thruster/actuator fault, we put that corresponding diagonal element in Γ matrix as zero. If there is no fault in any thruster/actuator, that corresponding diagonal entry of the fault-saturation matrix will be $1/\hbar_i$. Thus, it accounts for the force/torque saturation limits along with the fault information. We can rewrite Eq. (17) in terms of fault-saturation matrix, Γ, as

$$\nu = \Gamma\eta^T(\eta\Gamma\eta^T)^{-1}[\dddot{q}_d + K_1(\ddot{q}_d - \ddot{q}) + K_2(\dot{q}_d - \dot{q}) + K_3(\dot{q}_d - \dot{q})] - \gamma \tag{22}$$

Integration of Eq. (22) yields the desired thruster/ actuator force/torque as

$$F_{td} = \int \nu \, dt \tag{23}$$

2.4 Drag Minimization

Drag is a dissipative force that does not contribute to the motion. Actually, a UVMS will require a significant amount of energy to overcome the drag. Reduction of drag can also be useful from another perspective. The UVMS can experience a large reaction force because of the drag. High reaction force can saturate the controller and thus, degrade the performance of the autonomous system. Hence, we exploit the kinematic redundancy of the system not only to coordinate the motion of the UVMS but also to satisfy a secondary objective criterion that we believe will be useful in underwater applications. The secondary objective criterion that we choose to satisfy in this work is hydrodynamic drag optimization.

Recalling Eq. (6), we can write the complete solution to the joint-space acceleration as [22]:

$$\ddot{q}_{d_1} = J_{W_1}^{+}(\ddot{x}_{d_1} - \dot{J}\dot{q}_{d_1}) + (I - J_{W_1}^{+}J)\ddot{\phi}_1 \tag{24}$$

$$\ddot{q}_{d_2} = J_{W_2}^{+}(\ddot{x}_{d_2} - \dot{J}\dot{q}_{d_2}) + (I - J_{W_2}^{+}J)\ddot{\phi}_2 \tag{25}$$

where the null-space vectors $(I - J_{W_i}^{+}J)\ddot{\phi}_i$ (for *i=1,2*) are utilized to minimize the drag effects on the UVMS. We construct the vectors $\ddot{\phi}_i = -\kappa_i \nabla p^T$ (for *i=1,2*) applying Gradient Projection Method (GPM) on a scalar potential function of drag, $p(q,\dot{q})$, as $\nabla p(q,\dot{q}) = \partial p(q,\dot{q})/\partial q + \partial p(q,\dot{q})/\partial \dot{q}$. The positive constant κ_i is chosen considering the geometry and the dynamic characteristics of the subsystems of the UVMS. A detailed discussion can be found in [17].

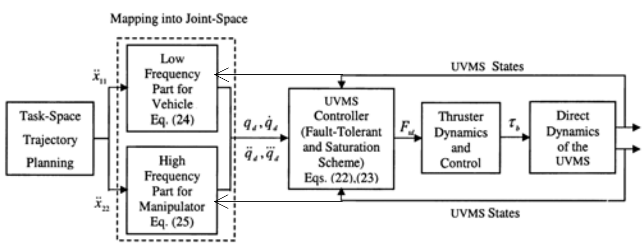

Figure 1: Unified dynamics-based motion planning scheme.

Thus, Eq. (24) and Eq. (25) provide us with the reference joint-space trajectories considering the dynamics-based planning method as well as the drag minimization scheme. Now, we can obtain all the desired join-space variables required for the control law (Eq. (22)) by integrating Eq. (24) and (25) and making use of Eq. (7). A block diagram of the proposed unified dynamics-based motion planning scheme is given in Figure 1.

3. Simulation Results

3.1 Trajectory

We have chosen a square planar path in xy (horizontal) plane for the computer simulation. We have assumed that each side of the square path is tracked in equal time. The geometric path and the task-space trajectories are given in Figure 2.

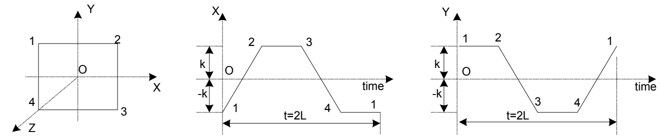

Figure 2: Task-space geometric path and trajectories.

The task-space trajectories can be represented as

$$x(t) = f_x(t) = \begin{cases} 4kt/L - k & \text{if } 0 < t \le L/2 \\ k & \text{if } L/2 < t \le L \\ 5k - 4kt/L & \text{if } L < t \le 3L/2 \\ -k & \text{if } 3L/2 < t \le 2L \end{cases} \tag{26}$$

$$y(t) = f_y(t) = \begin{cases} k & \text{if } 0 < t \le L/2 \\ 3k - 4kt/L & \text{if } L/2 < t \le L \\ -k & \text{if } L < t \le 3L/2 \\ 4kt/L - 7k & \text{if } 3L/2 < t \le 2L \end{cases} \tag{27}$$

$$z(t) = f_z(t) = 0 \tag{28}$$

The Fourier series for the above trajectories are as follows:

$$f_j(t) = a_{0j} + \sum_{r=1}^{\infty} a_{rj}\cos(r\pi t/L) + \sum_{r=1}^{\infty} b_{rj}\sin(r\pi t/L) \tag{29}$$

where '*j*' implies the coefficient for *x, y* or *z*; *k* is a constant and *2L* is the time period. The Fourier coefficients are $a_{0x} = -a_{oy} = k$, $a_{rx} = -a_{ry} = 4k/(r\pi)^2\ (\cos r\pi - 1)$ and $b_{rx} = -b_{ry} = 8k/(r\pi)^2\ \sin(r\pi/2)$.

For this simulation, we have taken *k= 1m,* i.e., the path is 2*m* square*, L=5* and maximum frequency at which the Fourier series is truncated is $r = p_1 = 30$. Total time of simulation = 10*sec*. The frequency of the manipulator is taken as 10 times higher than that of the vehicle. We have considered the natural frequency of the vehicle as 0.15 cycles per second and the manipulator to be 10 time faster than the vehicle. We have segmented the task space trajectories as

$$f_{j1}(t) = a_{0j} + a_{1j}\cos(\pi t/L) + b_{1j}\sin(\pi t/L) \tag{30}$$

$$f_{j2}(t) = \sum_{r=2}^{30} a_r\cos(r\pi t/L) + \sum_{r=2}^{30} b_r\sin(r\pi t/L) \tag{31}$$

3.2 Results and Discussion

We have performed extensive computer simulations to investigate the efficacy of the proposed Unified Dynamics-based Motion Planning (UDMP) algorithm. To verify the effectiveness of the proposed method, we have compared the results of UDMP approach with that of Conventional Motion Planning (CMP) method. In conventional method, the trajectory is designed in three sections: the main section (intermediate section) that is a straight line is preceded and followed by two short parabolic sections. The UVMS used for these simulations consists of a 6 dof vehicle and a 3 dof planar manipulator working in the vertical plane. The vehicle is ellipsoidal in shape with length, width and height 2*m*, 1*m* and 1*m*, respectively. The mass of the vehicle is 1073*kg*. The links are cylindrical and each link is 1*m* long. The radii of link 1, 2 and 3 are 0.1*m*, 0.08*m* and 0.07*m*, respectively. The link masses (oil filled) are 32*kg*, 21*kg* and 16*kg*, respectively. The simulation time is 10*sec* that is required to complete the square path. The total length of the path is 8*m*, thus the average speed is about 1.6*knot*. This speed is more than JASON vehicle (speed=1*knot*) but less than SAUVIM (Semi-Automated Underwater Vehicle for Intervention Mission) vehicle (designed speed=3 *knot*).

We have simulated two thruster faults: one horizontal thruster (Thruster 1) and the other one vertical thruster (Thruster 5). Both the thrusters stop functioning from 6*sec*. It is to be noted that both the thrusters are located at the same bracket of the UVMS, which is one of the worst thruster fault situations. In our simulation, we have considered the following thruster/actuator thrust/torque saturation limits: $\pm 400N$ for horizontal thrusters (Thruster 1-4), $\pm 200N$ for vertical thrusters (Thruster 5-8), $\pm 200N.m$ for actuator 1, $\pm 100N.m$ for actuator 2 and $\pm 50N.m$ for actuator 3. To make the simulation close to reality, we have introduced sensory noise in the measurements of positions and its derivatives. We have considered Gaussian noise of 1.0 mean and 1.0 standard deviation in the measurement of linear quantities (in *mm* unit), and 0.01 mean and 0.05 standard deviation in measurement of angular quantities (in *deg* unit). We have considered 10% modeling inaccuracy during computer simulation to reflect the uncertainties that are present in underwater environment. Thruster dynamics have been incorporated into the simulation using the thruster dynamics described in [23].

We have presented results from the computer simulations in Figure 3 through Figure 7. The results we have provided here are from Case I: *Partial Decomposition* of the proposed UDMP method. The task-space geometric paths are plotted in Figure 3, where we can see that the path tracking errors in our proposed UDMP method are much smaller as compared to that of CMP method. It is also observed from Figure 4 that the end-effector tracks the task-space trajectories quite accurately in UDMP method. The errors are very large in CMP method as compared to the proposed method. The joint-space trajectories are plotted in Figure 5. From these plots it is observed that the proposed UDMP method effectively reduces the motions of the heavy subsystem (the vehicle) and allows greater and sharper motions to the lighter subsystem (the manipulator) while tracking the same task-space trajectories. It is also noticed that the motion of the heavy subsystem is smoother in the proposed method. We find that these sharper and larger motions of the heavy subsystem in case of CMP method demand higher driving force that we see in Figure 6. From the plots in this figure it is also observed that in case of UDMP method thrusters 4,7,8 and actuator 1 have reached the saturation limits, but they have not exceeded the limits. On the other hand, in case of CMP method all the thrusters and actuators have reached the saturation limits, however the saturation scheme has not allowed them to cross the limits. This, in turn, degrades the trajectory tracking performance in CMP method as we can see in Figure 3 and Figure 4. Thus, the conventional planning method demands more powerful actuation system to track the same trajectories with reasonable accuracy. We observe that the thrust 1 and thrust 5 are zero from 6*sec* as marked by “A” and “B”, respectively. These imply they have developed faults. At this moment we observe some perturbations in trajectories and paths, however, the UDMP scheme gradually brings the system to the desired directions.

We have also plotted the simulation results for surge-sway motion, power requirement and energy consumption of the UVMS in case of CMP method (in the left column) and that of in case of proposed UDMP method (in the right column) in Figure 7. Top two plots in this figure show the profile of the surge- sway movements of the vehicle in the said two methods. In case of the CMP method, the vehicle changes the motion sharply and moves more as compared to the motion generated from the UDMP method. It may so happen that this type of sharp movements may be beyond the capability of the heavy dynamic subsystem and consequently large errors in trajectory tracking will occur. Additionally, this may cause saturation of the thrusters and the actuators. Moreover, the vehicle will experience large velocity and acceleration in CMP method that results in higher power requirement and energy consumption, as we observe in next two sets of plots in Figure 7. Thus, this investigation reveals that our proposed Unified Dynamics-based Motion Planning (UDMP) method is quite promising for autonomous operation of a UVMS.

4. Conclusions

We have proposed a new unified dynamics-based trajectory planning algorithm that can generate both kinematically admissible and dynamically feasible joint-space trajectories for systems composed of heterogeneous dynamics. We have then extended this algorithm for an autonomous underwater vehicle-manipulator system, where the dynamic response of the vehicle is much slower than that of the manipulator. We have also exploited the kinemetic redundancy to accommodate the thruster/ actuator faults, saturation and, also to minimize hydrodynamic drag. We have considered and thruster dynamics when modeling the UVMS. The results from computer simulations demonstrate the effectiveness of the proposed method. It shows that the proposed algorithm can significantly reduce the energy and the power requirements for autonomous operation of a UVMS. We did not present results from Case II (*Total Decomposition*) simulations because of lack of space. However, those results are also better than that from the conventional technique. A systematic study is currently underway to assess the relative merits between Case I and Case II.

There are a few drawbacks of this paper as well. We used a model-based control technique to evaluate our planning algorithm. However, the underwater environment is uncertain and we need to use adaptive control techniques in future. Finally, the proposed scheme needs to be validated by experiments. We are currently working on these deficiencies. We hope to conduct experiments on SAUVIM (or similar system), which is an underwater vehicle having one 7 dof electrically powered Ansaldo arm, currently being developed at the University of Hawaii.

Acknowledgments

This work was partially supported by the National Science Foundation under grant BES97-01614 and the Office of Naval Research under grant N00014-97-1-0961.

References

[1] C. A. Klein, and C. H. Huang, "Review of Pseudoinverse Control for Use with Kinematically Redundant Manipulators," *IEEE Trans. on Sys, Man and Cyber.*, Vol. SMC-13, No. 3, pp. 245-250, 1983.

[2] R. Paul, "Manipulator Cartesian Path Planning," *IEEE Transactions on Systems, Man and Cybernetics*, Vol. SMC-9, No. 11, pp. 702-711, 1979.

[3] Z. L. Zhou, and C. C. Nguyen, "Globally Optimal Trajectory Planning for Redundant Manipulators using State Space Augmentation Method," *J. of Intelligent and Robotic Sys.*, Vol. 19, No. 1, pp. 105-117, 1997.

[4] B. Siciliano, "Closed-Loop Inverse Kinematics Algorithms for Redundant Spacecraft/Manipulator Systems," in the *Proc. of IEEE Int. Conf. on Robotics and Automation,* pp. 95-100, Atlanta, GA, 1993.

[5] G. Antonelli, and S. Chiaverini, "Task-Priority Redundancy Resolution for Underwater Vehicle-Manipulator Systems," in the *Proc. of IEEE Int. Conf. on Robotics and Automation,* pp. 756-761, Leuven, Belgium, May 1998.

[6] M. Vukobratovic, and M. Kircanski, "A Dynamic Approach to Nominal Trajectory Synthesis for Redundant Manipulators," *IEEE Trans. on Sys., Man, and Cyber.*, Vol. SMC 14, No. 4, pp. 580-586, 1984.

[7] J.E. Bobrow, "Optimal Robot Path Planning Using the Minimum-Time Criterion," *IEEE J. of Robotics and Automation*, Vol. 4, No. 4, pp. 443-450, August 1988.

[8] Z. Shiller, and S. Dubowsky, "Robot Path Planning with Obstacles, Actuator, Gripper, and Payload Constraints," the *International Journal of Robotics Research*, Vol. 8, No. 6, pp. 3-18, December 1989.

[9] K. Shin, and N. McKay, "A Dynamic programming Approach to Trajectory Planning of Robot Manipulators," *IEEE Transactions on Automatic Control*, Vol. AC-31, No. 6, pp. 491-500, June 1986.

[10] A.R. Hirakawa, and A. Kawamura, "Trajectory Planning of Redundant Manipulators for Minimum Energy Consumption without Matrix Inversion," in the *Proceedings of the IEEE Int. Conf. on Robotics and Automation,* pp. 2415-2420, Albuquerque, NM, April 1997.

[11] S. F. P. Saramago, and V. Steffen Jr., "Optimization of the Trajectory Planning of Robot Manipulators Taking into Account the Dynamics of the System," *Journal of Mechanism and Machine Theory*, Vol. 33, No. 7, pp. 883-894, 1998.

[12] S. Macfarlane, and E. A. Croft, "Jerk-bounded Manipulator Trajectory Planning: Design for Real-time Applications," *IEEE Transactions on Robotics and Automation*, Vol. 19, No. 1, pp. 42-52, Feb. 2003.

[13] N. Faiz, and S.K. Agrawal, "Trajectory Planning of Robots with Dynamics and Inequalities," in *the Proc. of IEEE Int. Conf. on Robotics and Automation*, pp. 3977-3983, San Francisco, CA, April 2000.

[14] O. Brock, and O. Khatib, "High-Speed Navigation Using the Global Dynamic Window Approach," in the *Proc. of the IEEE Int. Conf. on Robotics and Automation,* pp. 341-346, Detroit, MI, May 1999.

[15] Y. Yamamoto, and S. Fukuda, "Trajectory Planning of Multiple Mobile Manipulators with Collision Avoidance Capability," in the *Proc. of the IEEE Int. Conf. on Rob. and Auto.*, pp. 3565-3570, May 2002.

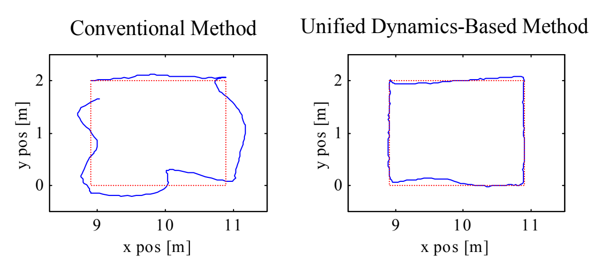

Figure 3: Task-space geometric paths: Conventional method in the left and Unified Dynamics-Based method in the right. Doted/red lines denote the desired paths and solid/blue lines denote actual paths.

[16] D. R. Yoerger, and J. J. E. Slotine, “Robust Trajectory Control of Underwater Vehicles,” *IEEE J. of Oceanic Eng.*, Vol. 10, No. 4, pp. 462-470, October 1985.

[17] N. Sarkar and T.K. Podder, “Coordinated Motion Planning and Control of Underwater Vehicle-Manipulator Systems Subject to Drag Optimization,” *IEEE J. of Oceanic Engineering*, Vol. 26, No. 2, pp. 228-239, 2001.

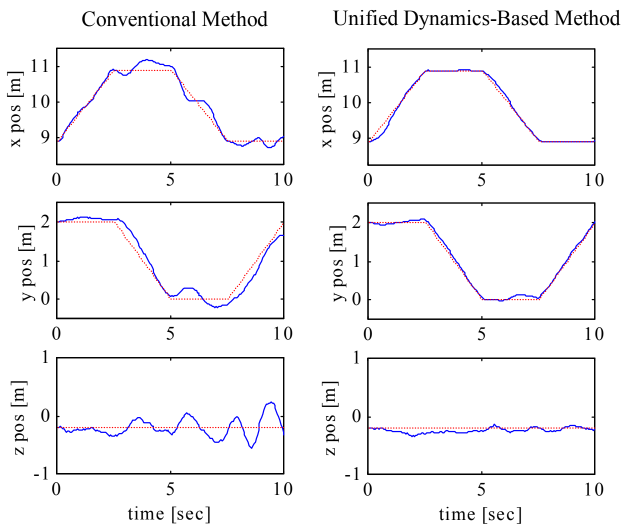

Figure 4: Task-space trajectories: Conventional method (left column) and Unified Dynamics-Based method (right column). Actual trajectories (solid/blue lines) are superimposed on desired trajectories (dash/red lines).

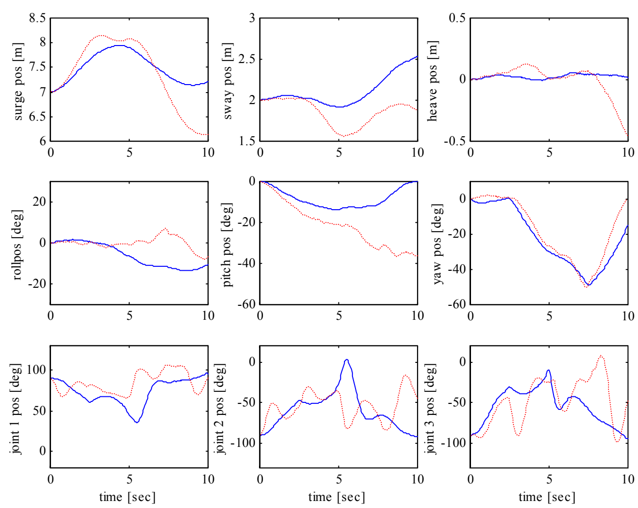

Figure 5: Joint-space trajectories: Unified Dynamics-Based method (solid/blue lines) and Conventional method (dash/red).

[18] A.J. Healy, and D. Lienard, “Multivariable Sliding-mode for Autonomous Diving and Steering of Unmanned Underwater Vehicles,” *IEEE J. of Oceanic Engineering*, Vol. 18, No. 3, pp. 327-339, 1993.

[19] T.K. Podder, and N. Sarkar, “Fault Tolerant Control of an Autonomous Underwater Vehicle Under Thruster Redundancy: Simulation and Experiments,” in the *Proc. of IEEE Int. Conf. on Robotics and Automation*, pp.1251 -1256, San Francisco, April 2000.

[20] T.K. Podder, G. Antonelli, and N. Sarkar, “An Experimental Investigation into the Fault-tolerant Control of an Autonomous Underwater Vehicle,” *Advanced Robotics Journal*, Vol. 15, No. 5, pp. 501 - 520, 2002.

[21] A. Isidori, C.H. Moog, and A. De Luca, “A Sufficient Condition for Full Linearization via Dynamic State Feedback,” in the *Proc. of IEEE Conf. on Decision and Control*, pp. 203-208, Athens, Greece, Dec. 1986.

[22] Y. Nakamura, “*Advanced Robotics: Redundancy and Optimization*,” Addison-Wesley Pub. Co., 1991.

[23] A.J. Healey, S.M. Rock, S. Cody, D. Miles and J.P. Brown, “Toward an Improved Understanding of Thruster Dynamics for Underwater Vehicles,” *IEEE J. of Oceanic Eng.*, Vol. 20, No. 4, pp. 354-361, 1995.

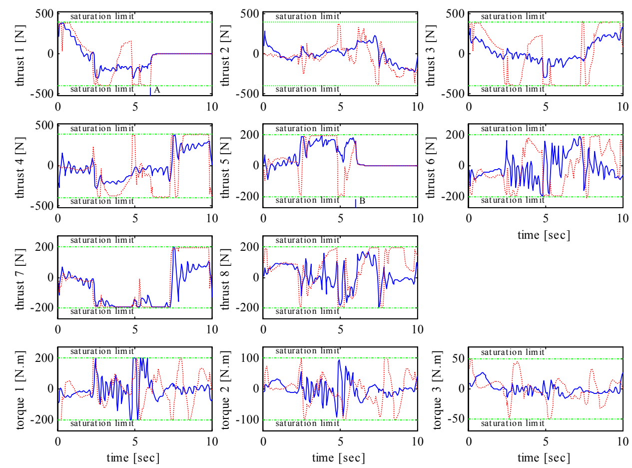

Figure 6: Thruster and actuator forces and torques of the UVMS. Unified Dynamics-Based method (solid/blue lines) and Conventional method (dash/red lines). Thruster faults are marked by “A” (Thruster 1) and “B” (Thruster 5).

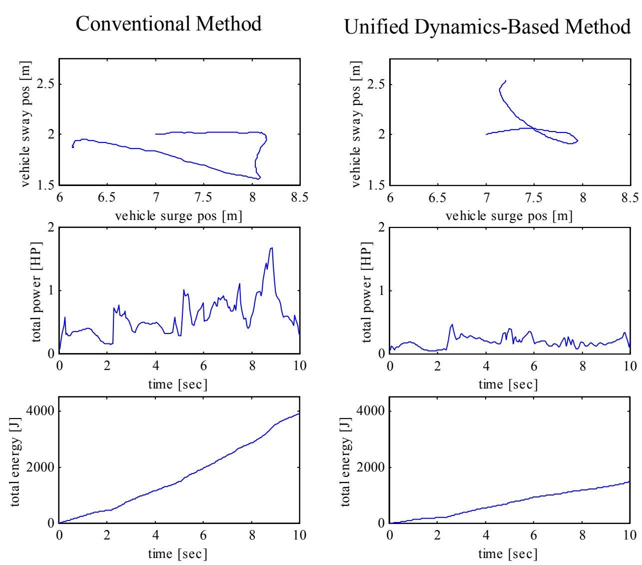

Figure 7: Surge-sway motion of the vehicle, power requirement and energy consumption of the UVMS. Results from Conventional method are in the left and that of Unified Dynamics-Based method are in the right.